1st Croatian Conference on Earthquake Engineering
1CroCEE
22-24 March 2021 Zagreb, Croatia

DOI: https://doi.org/10.5592/CO/1CroCEE.2021.79

# Study of ground amplification characteristics by strong motion and microtremor observations – A simple study on ground nonlinearity by equivalent linear analysis

**Tsutomu Ochiai[1], Takahisa Enomoto[2], Shigeki Senna[3]**

[1] Kanagawa University, Dept. of Architecture and Building Engineering, *ochiai@kanagawa-u.ac.jp*
[2] Kanagawa University, Dept. of Architecture and Building Engineering, *enomot01@kanagawa-u.ac.jp*
[3] National Research Institute for Earth Science and Disaster Resilience, *senna@bousai.go.jp*

## Abstract

On June 18, 2019, there was a magnitude 6.7 earthquake at a depth of about 15 km off the coast of Yamagata Prefecture. A seismic intensity [Japan Meteorological Agency Seismic Intensity Class; JMA] of 6+ [larger] was observed in Murakami City, Niigata Prefecture, and a seismic intensity of 6- [smaller] was observed in Tsuruoka City, Yamagata Prefecture. The authors conducted a damage survey from June 29 to July 1 after the earthquake and conducted microtremor array observations at nine points centred on the strong motion observation points in October. The ground structure [layer thickness and Shear wave velocity] of the surface layer was estimated from the observation of the microtremor array and compared with the existing ground structure. In addition, a comparison of the ground amplification characteristics obtained from the ground structure and the strong motion observation records could be divided into three groups. That is, a group that is consistent and has a peak in a short period of 0.2 s or less. Consistent group with peaks around 0.2-0.4s. A group in which the predominant period of strong motion records is slightly longer. Therefore, a simple study using equivalent linear analysis was carried out in order to consider the non-linearity of the ground. As a result, considering the non-linearity of the ground, the result can be explained including the group with a long period of predominance.

***Key words:*** strong motion observation, microtremor observation, amplification characteristics, nonlinearity

## 1 Introduction

On June 18, 2019, there was an earthquake of magnitude 6.7 at a depth of about 15 km off the coast of Yamagata Prefecture. Seismic intensities [JMA] of 6+ [larger] and 6- [smaller] were recorded in Murakami City, Niigata Prefecture and Tsuruoka City, Yamagata Prefecture, respectively.

Along the Sea of Japan, large earthquakes have occurred many times near the present hypocenter: the 1833 Shonai-Oki Earthquake (M:7.4), the 1964 Niigata Earthquake (M:7.5), and the 1983 Sea of Japan Earthquake (M:7.7). On land, the 1894 Shonai Earthquake with the hypocenter located in the Shonai Plain in the north (M:7.0) led to major damages with 726 deaths, 987 injuries, 3858 homes destroyed, and 2148 homes burned [1, 2]. Photographs show old wooden homes (some with thatched roof) that were completely destroyed [3].

Authors conducted a survey of the damage between June 29 - 11 days after the Earthquake- and July 1 [4]. In October of the same year, authors confirmed the reconstruction stage and observed microtremors around the point of the strong seismic motion observation. Using the summary of the damages and routine microtremor observations and strong seismic motion observations, authors examined ground amplification characteristics especially for the shallow zone [about GL- 50 m].

## 2 Summary of seismic damages

Table 1 shows the list of damages to people and buildings (residential buildings and non-residential buildings). Damages were concentrated in Yamagata Prefecture and Niigata Prefecture, where majority of damages was focused around Tsuruoka City, Yamagata Prefecture and Murakami City, Niigata Prefecture [5, 6]. Immediately after this Earthquake, there was a tsunami with the highest wave of 11 cm in Nezugaseki, Tsuruoka City.

The damage survey confirmed damages to buildings mainly around the point of strong seismic motion observation. Damage to roof tiles was quite notable in Koiwagawa, Tsuruoka City near the hypocenter (Figure 2, KOIWAGAWA). Damages to roof tiles in Koiwagawa were observed in about 30 % of roofs in our visual observation, which was consistent with aerial photographs taken by Geospatial Information Authority of Japan [7] and other damage surveys [8]. In hot spring areas near the epicenter (Figure 2, YMT004), we surveyed the ratio of headstones that fell in two cemeteries. It was about 30 % in Chotokuji and about 10 % in Atsumi Hot Spring community cemetery, which was consistent with the measured seismic intensity [9, 10].

**Table 1. List of seismic damages**

| □ | Parsonal damage (People) | | Residential damege (Building) | | | Non-residential damege (Building) | |
|---|---|---|---|---|---|---|---|
| | Serious | Minor | Complete collapse | Half collapse | Partially collapse | Public | Other |
| Miyagi pref. | □ | 5 | □ | □ | □ | □ | □ |
| Akita pref. | 1 | 1 | □ | □ | 1 | □ | 1 |
| Yamagata pref. | 3 | 25 | □ | 4 | 940 | □ | 5 |
| Niigata pref. | 4 | 3 | □ | 24 | 639 | □ | □ |
| Ishikawa pref. | 1 | □ | □ | □ | □ | □ | □ |
| Total | 9 | 34 | 0 | 28 | 1580 | 0 | 6 |


**Figure 1. The sample of fallen headstones**

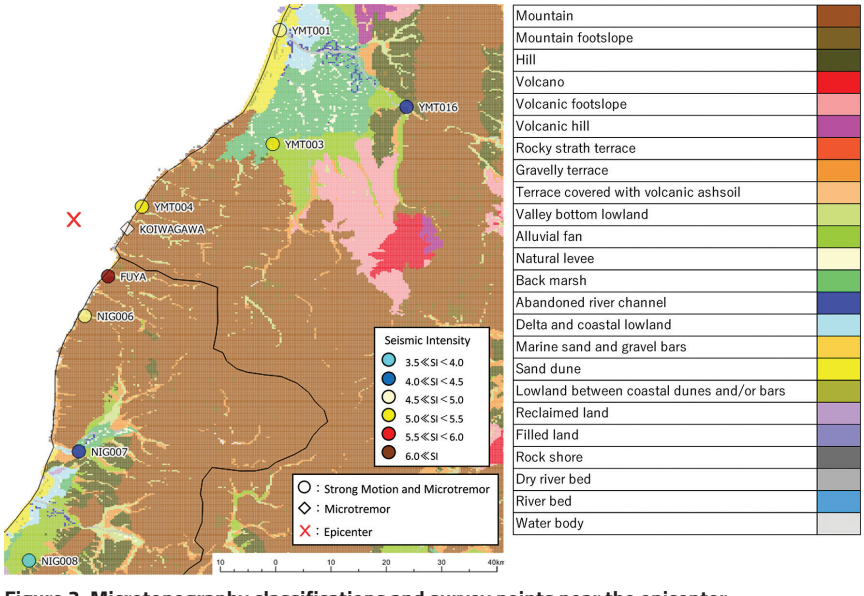


**Figure 2. Microtopography classifications and survey points near the epicenter**

## 3 Geomorphology / geology and observation points of strong seismic motion

The microtopography classification (J-SHIS, 250-m mesh) near the hypocenter is shown in Figure 2. The Figure also shows the epicenter and survey points (measured seismic intensity for observation points of strong seismic motion). The hypocenter was off the coast near the boundary between Niigata Prefecture and Yamagata Prefecture, and the closest land area is mountainous. This mountainous area has narrow dendritic plateaus and lowlands, and nearby survey points mostly are located in dendritic plateaus or lowlands (YMT004, KOIWAGAWA, FUYA, NIG006).

In the north side of the mountainous area, Shonai Plain was developed by Mogami River and Aka River. YMT016 is located in the fan where the landscape of the Mogami River basin changes from mountains to lowlands, while YMT001 is located in a sand dune near the mouth. YMT003 is located near the edge of a fan in the Aka River basin.

In the south side of the mountainous area, Shinano River and Agano River have formed the Echigo Plain. The northern part of Niigata Prefecture that we surveyed is located in the northern edge of the Echigo Plain. Two points of observations for strong seismic motions are both located in fans near the boundary between mountainous area and lowlands (NIG007, NIG008).

## 4 Records of strong seismic motions and microtremors and ground amplification characteristics

### 4.1 Ground structure

In the present study, ground amplification characteristics were examined in nine locations: seven locations near strong seismic motion observation made by K-NET in northern Niigata Prefecture and southern Yamagata Prefecture shoreline, one location near a seismic intensity measurement point for Japan Meteorological Agency (FUYA), and one near Koiwagawa, Tsuruoka City, where seismic damage was notable (KOIWAGAWA). At each point, microtremor array observation (two arrays with radius of 0.6 m and 10 m) [11] was performed. S wave structures obtained from the observation are shown in Figure 3. K-NET observation points in the Figure include published S wave structures and S wave structures calculated from N value [12]. Overall, values are consistent, but there are slightly different trends at YMT003 and NIG006. At YMT003, array observation shows a layer with low Vs at depth (Vs obtained from N is consistent with array observation). In contrast, at NIG006, PS log shows a layer with low Vs at depth (Vs obtained from N is consistent with PS log).

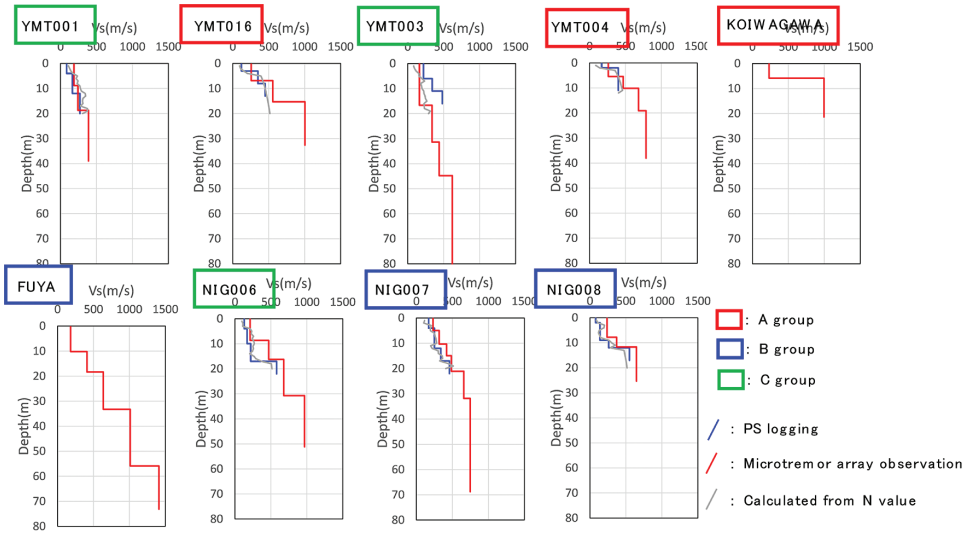


**Figure 3. S wave structure at the survey points**

## 4.2 Examination of ground amplification characteristics

From Vs structure (PS log and microtremor array), we calculated a ground transfer function that assumes vertically incident S wave [13]. In addition, for the microtremor H/V spectral ratio (MHVR), 20.48 seconds were isolated from the observation results from the center of the array, which was smoothed with Parzen window with the band width of 0.3 Hz. H/V spectral ratio of seismic intensity record (June 18, 2019) obtained through smoothing in the same manner as microtremors (EMHVR) and transfer function are shown in Figure 4. If ground structures by PS logging and microtremor array are the same, transfer function and predominant period of MHVR and EHVR would be generally agree, being consistent to existing results [14]. We classified the results into three groups, A, B, and C, based on the spectral characteristics. Comparing with the ground structures in Figure 3, we can confirm the corresponding relationship between ground and spectral characteristics.

A: All peaks in short periods of 0.2 seconds of less

Locations: YMT016, YMT004, (KOIWAGAWA)*

Ground: → Vs ≥ 400 m/s at 10 m to the surface

B: Generally, peaks with periods of 0.2 to 0.4 seconds

Locations: FUYA, NIG007, NIG008

Ground: Vs ≥ 400 m/s from 10 m down

C: Only peaks of strong seismic motions or long periods

Locations: YMT001, YMT003, NIG006

Ground: Soft with Vs ≤ 200 m/s in the top 10 m

*: KOIWAGAWA was judged based on the result of microtremor only

## 4.3 Impact of ground nonlinearity based on seismic record

In the group C, compared to MHVR, peaks of EMHV were shifted toward longer periods. A reason for this is the nonlinearity of the ground. Here, we attempted an analysis with seismic record with different sizes of seismic motion. Table 2 show maximum acceleration of the present earthquake (synthesized), measured seismic intensity, and AVS30 obtained from microtremor array. Table2 shows that the group C has higher measured seismic intensity compared to other observation points. We assumed that the ground has become nonlinear with the input of large seismic motion, and obtained and compared EHVR from seismic motion data with small input for three locations in group C. We focused on the measured seismic intensity for seismic motion, and randomly selected about ten seismic motions each for seismic intensity of 3 to 4, 1 to 2, and 0.5 or below. We obtained the mean spectrum from each EMHV (Figure 5).

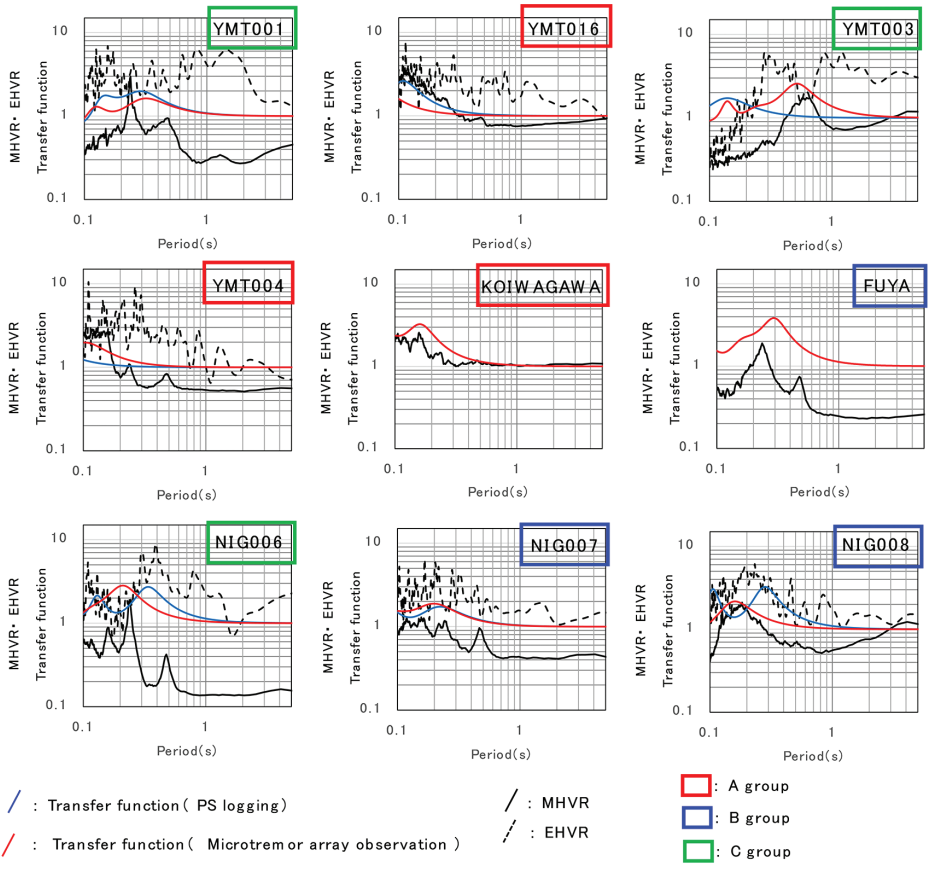


**Figure 4. Spectral characteristics of survey points**

At YMT003 and NIG006, EHVR from June 18, 2019 was shifted to a somewhat longer period, indicating the impact of nonlinearity of the ground. At YMT001, however, a clear difference could not be confirmed. At this point, compared to other points near the mouth of Mogami River, soft and weak ground is relatively thick, and sand becomes more dominant as the area is dominated by sand dunes. Since the existing microtremor observation results [15] and spectral characteristics are different, it is possible that the result of microtremor observations is unique. We plan to conduct detailed examination at a later date.

**Table 2. Seismic record (June 18, 2019) and ground at observation points**

| □ | No. | PGA [gal] | SI | Epicenter Dist. [km] | AVS30* [m/s] |
|---|---|---|---|---|---|
| A | YMT016 | 175.9 | 4.1 | 51 | 530 |
| | YMT004 | 653.4 | 5.2 | 10 | 519 |
| | KOIWAGAWA | - | - | 8 | 601 |
| B | FUYA | 1191.3 | 6.1 | 12 | 317 |
| | NIG007 | 145.4 | 4.2 | 42 | 475 |
| | NIG008 | 88.3 | 3.7 | 62 | 416 |
| C | YMT001 | 102.0 | 4.5 | 45 | 258 |
| | YMT003 | 269.8 | 5.3 | 31 | 210 |
| | NIG006 | 250.6 | 4.8 | 17 | 391 |
| *AVS30 is calculated from microtremor array observation | | | | | |

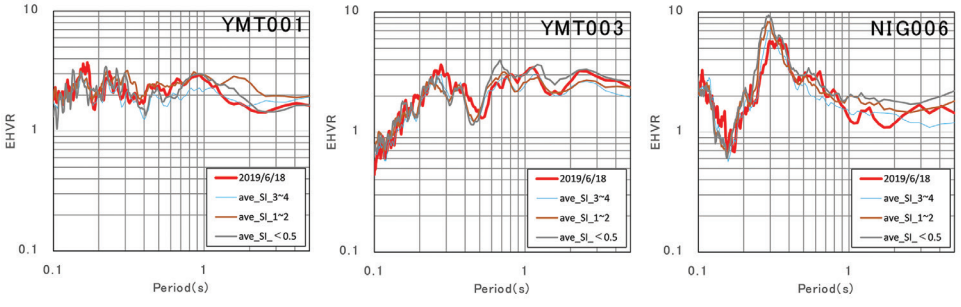


**Figure 5. Changes in EHVR due to the size of seismic motions (C group)**

## 4.4 Impact of ground nonlinearity in numerical simulations

In Section 4.3, we examined the impact of ground nonlinearity based on actual observation record. We conducted an equivalent linear analysis of the ground. The equivalent linear analysis was conducted with SHAKE. For the setting of nonlinearity of the ground, laboratory soil test is ideal. However, such laboratory soil test was not conducted for the target area. Thus, referring to papers presented by Architectural Institute of Japan [16],

such as Koyamada et al. [17], we distinguished sand and clay. Nonlinearity of each type of soil is shown in Figure 6.

A flowchart of the study is shown in Figure 7. We set the above-describe nonlinearity relative to the linear model used to obtain the transfer function. On the other hand, we analysed the ground record of the present Earthquake again to obtain the seismic motion of the bedrock. Using a model of the bedrock seismic motion and nonlinearity, we conducted the equivalent linear analysis and obtained the transfer function of the bedrock and the ground surface. Figure 8 shows the transfer function of the linear model and the transfer function of the equivalent linear model that uses the present seismic record.

The Figure shows that Group B with little difference in peak periods of MHVR and EHVR had nearly the same transfer function in the present examination. On the other hand, in Group C with a longer period for EHVR compared to MHVR, the equivalent linear analysis had a longer period than the linear analysis, confirming a similar trend.

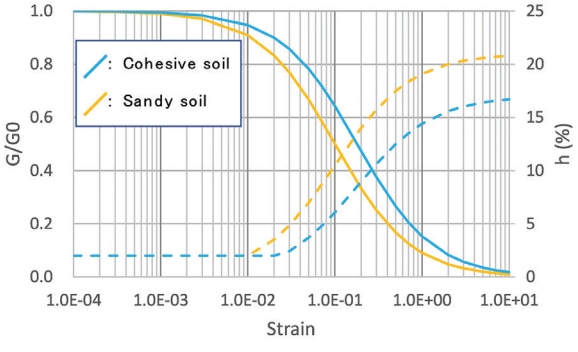


**Figure 6. Strain-dependent characteristics used in the analysis**

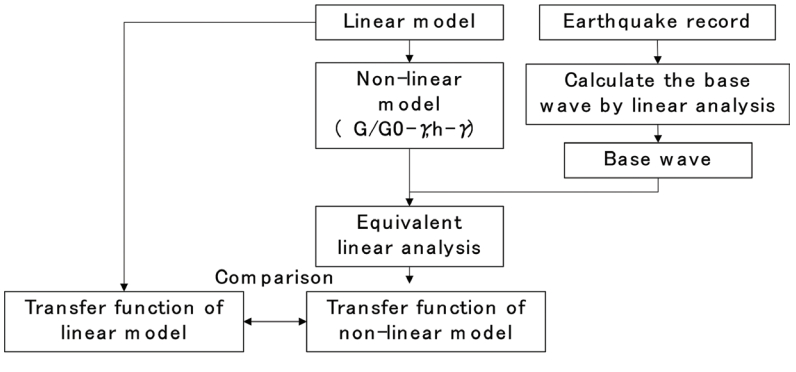


**Figure 7. Flowchart of an equivalent linear analysis**

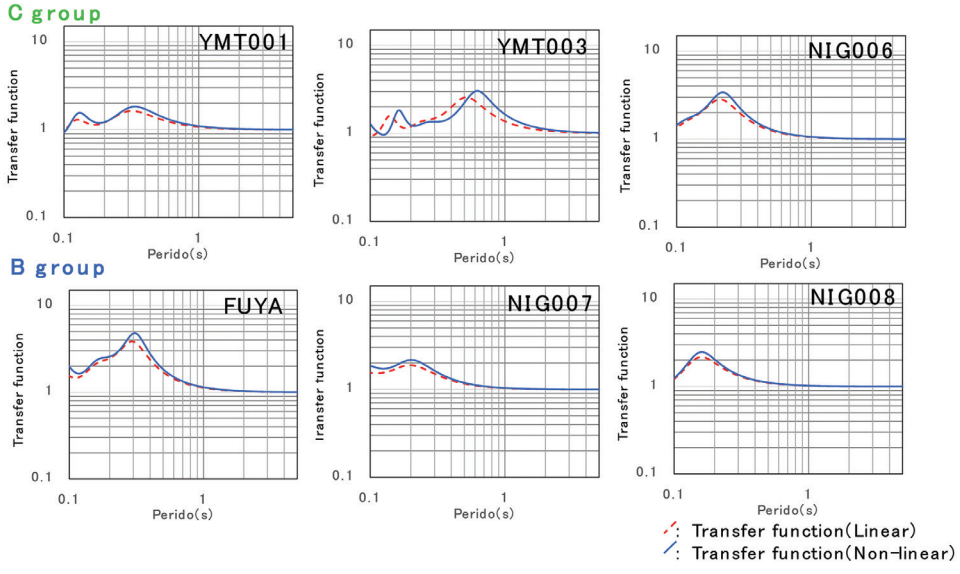


**Figure 8. Test result of an equivalent linear analysis**

## 5 Conclusions

We summarized the damages from the 2019 Yamagata Earthquake that occurred on June 18. We examined ground amplification characteristics using microtremor observations and so on. The results are summarized below:

- Koiwagawa, where the seismic damage was most notable, has a bedrock characterized by short period.
- Areas of short-period ground tend to have large acceleration. If the acceleration is large, the damage caused by flying objects will increase.
- This result is consistent with the main seismic destruction being damage to tile roofs.
- Through observations of strong seismic motions and the equivalent linear analysis, we confirmed that the vibration characteristics changed due to nonlinearity of the ground.

## Acknowledgement

For recording strong seismic motion, we used the records of K-NET and KiK-net (National Research Institute for Earth Science and Disaster Resilience) and Japan Meteorological Agency. During the field work, we received many advices from honorary professor Takahiro Iwatate of Tokyo Metropolitan University, who accompanied us. We would like to extend our most sincere appreciation.

## References


[1] Yamagata Prefecture (2006): Yamagata Prefecture Seismic Damage Estiamte Survey — the western marginal fault zone of Nagai Basin and Shonai Plain fault zone — Survey report

[2] Mizuta, T., Kagami, H. (2013): Literature survey on the distribution of damage from October 22, 1894 Shonai Earthquake by sections of villages, AIJ Journal of Technology and Design, Vol. 19, no. 43, pp. 1235-1238

[3] Osako, M. (2005): Photographic documents from the 1894 Shonai Earthquake and the 1896 Rikuu Earthquake, Bull. Natn. Sci. Mus., Tokyo, Ser. E, 28, pp. 1-11

[4] Ochiai, T., Enomoto, T., Senna, S. (2020): Examination of seismic damages off the coast of Yamagata Prefecture in June 2016 and ground vibration characterstics, the 48th Ground Motion Symposium (2020), pp. 49-52

[5] FDMA Energency Response Room (2020): Damages from the earthquake with the hypocenter off the coast of Yamagata Prefecture and response by fire and rescue department (no. 19)

[6] Cabinet Office (2019): Damages from the earthquake with the hypocenter off the coast of Yamagata Prefecture

[7] Geospatial Information Authority of Japan (2020): Information regarding the 2019 Earthquake off the coast of Yamagata Prefecture, https://www.gsi.go.jp/BOUSAI/R1_yamagatakenoki_earthquake.html, (accessed 1 October 2020)

[8] Mitsuji, K., Ono, S. (2019): Preliminary survey of the Earthquake off the coast of Yamagata Prefecture on June 18, 2019, and routine microtremor observations, Japan Association for Earthquake Engineering Annual Meeting

[9] Tomozawa, Y., Motoki, K., Kato, K., Hikita, T., Ishiki, K. (2017): Investigation of tombstones fall-down rates and damages of wooden houses due to the 2016 Kumamoto Earthquake: - comparative examination of near-fault region and Mashiki-machi Miyazono, Journal of Japan Association for Earthquake Engineering, Vol. 17, no. 4, pp. 62-80, doi: https://doi.org/10.5610/jaee.17.4_62

[10] Miyano, M. (1982): Some investigations on the seismic intensity supposed from overturning of gravestones, damages of wooden houses and others, Proceedings of the Japan Society of Civil Engineers, no. 319, pp. 33-42 doi: https://doi.org/10.2208/jscej1969.1982.319_33

[11] Cho, I., Senna, S. (2016): Constructing a system to explore shallow velocity structures using a miniature microtremor array: Accumulating and utilizing large microtremor datasets, Synthesiology, Vo.9, No.2, pp. 86-96, doi: https://doi.org/10.5571/synth.9.2_86

[12] Ota, Y., Goto, N. (1978): Experimental formula to estimate transverse wave velocity and physical background, Geophysical Exploration, Vol. 31, no. 1, pp. 8-17

[13] Senna, S., Fujiwara, H. (2008): Development of analyzing tools for microtremor survey observation data, Vol. 1 - tools for analysis of microtremor data, National Research Institute for Earth Science and Disaster Resilience document, Vol. 313

[14] Nagao, T., Yamada, M., Nozu, A. (2012): A study on the interpretation of wave components in microtremor H/V spectrum, Journal of Japan Society of Civil Engineers Ser. A1 (Structural Engineering and Earthquake Engineering), Vol.68, No.1, pp. 48-62, doi: https://doi.org/10.2208/jscejseee.68.48

[15] Mizuta, T., Kagami, H. (2015): Relation between damage of wooden huoses during the 1894 Shonai Earthquake and H/V spectral ratio of microtremors, Tohoku Journal of Natural Disaster Science, Vol. 51, pp. 155-158

[16] Architectural Institute of Japan (2007): Response analysis and seismic design that consider dynamic interaction between buildings and the ground

[17] Koyamada, K., Miyamoto, Y., Miura, K. (2003): Nonlinear property for surface strata from natural soil samples, Proceedings of the Japan National Conference on Geotechnical Engieering, JGS 38, pp. 2077-2078, doi: https://doi.org/10.11512/jiban.JGS38.0.2077.0